Triplet–triplet energy transfer in fucoxanthin-chlorophyll protein from diatom *Cyclotella meneghiniana*: Insights into the structure of the complex

Marilena Di Valentin [a], Elena Meneghin [a], Laura Orian [a], Antonino Polimeno [a], Claudia Büchel [b], Enrico Salvadori [c], Christopher W.M. Kay [c], Donatella Carbonera [a],*

[a] *Department of Chemical Sciences, University of Padua, via Marzolo 1, 35131 Padova, Italy*
[b] *Max-Planck Institute of Biophysics, Marie-Curie Strasse 13-15, D-60439 Frankfurt, Germany*
[c] *Institute of Structural and Molecular Biology and London Centre for Nanotechnology, University College London, Gower Street, London WC1E 6BT, UK*

ABSTRACT

Although the major light harvesting complexes of diatoms, called FCPs (fucoxanthin chlorophyll a/c binding proteins), are related to the *cab* proteins of higher plants, the structures of these light harvesting protein complexes are much less characterized. Here, a structural/functional model for the "core" of FCP, based on the sequence homology with LHCII, in which two fucoxanthins replace the central luteins and act as quenchers of the Chl a triplet states, is proposed. Combining the information obtained by time-resolved EPR spectroscopy on the triplet states populated under illumination, with quantum mechanical calculations, we discuss the chlorophyll triplet quenching in terms of the geometry of the chlorophyll–carotenoid pairs participating to the process. The results show that local structural rearrangements occur in FCP, with respect to LHCII, in the photoprotective site.

© 2013 Elsevier B.V. All rights reserved.

1. Introduction

Diatoms are unicellular, eukaryotic algae which play an important role in the climate of both marine and freshwater environments. The organization of the photosynthetic apparatus of diatoms, plants, and red algae is very similar, but, at the same time, there are significant differences in membrane topology, and in polypeptide and pigment composition. The thylakoid membranes are not differentiated into grana and lamellae and there is no spatial separation of photosystem (PS) I and PS II [1]. Moreover, in contrast to higher plants and green algae, the light-harvesting complexes of diatoms contain chlorophyll (Chl) c instead of Chl b, and fucoxanthin (Fx), instead of lutein, as the major carotenoid (Car) (the structures of the two carotenoids are reported for comparison in Fig. 1). These light harvesting complexes, called FCPs (fucoxanthin chlorophyll a/c binding proteins), are related to the *cab* proteins of higher

plants [2–4]. Although the homologies are significant, the polypeptides in FCPs are smaller in size (17–23 kDa) and the proteins are expected to be more hydrophobic.

FCPs have been isolated in different oligomeric states from *Cyclotella meneghiniana*, with a preferential organization of 18 kDa proteins into trimers and of 19 kDa polypeptides into higher oligomeric states [5,6]. This oligomerization marks a difference in the supramolecular structure of the FCP proteins compared to that of LHCII, likely reflecting the different arrangements of the thylakoid membranes [5]. The major xanthophyll cycle pigments in diatoms are diadinoxanthin and diatoxanthin. The localization of these pigments within the FCP light-harvesting complexes has been demonstrated and it has been shown that diatoxanthin plays an active role in non-photochemical quenching (NPQ) [6–10]. Thus, as LHCII of higher plants, FCP functions both in light harvesting and photoprotection. As suggested by the sequence homology, FCP is inserted in the membrane by three membrane spanning α-helixes, as the LHCII polypeptides in higher plants. The similarity is especially strong in helixes 1 and 3 [11], but mature FCPs have been found to be smaller in size than the plant LHCs, due to shorter loops and termini [11–13]. Compared to higher plants, green algae, and photosynthetic bacteria, the structures of the protein complexes and the molecular mechanisms of the photo-physical processes occurring in the light-harvesting complexes of diatoms have been explored in much less detail.
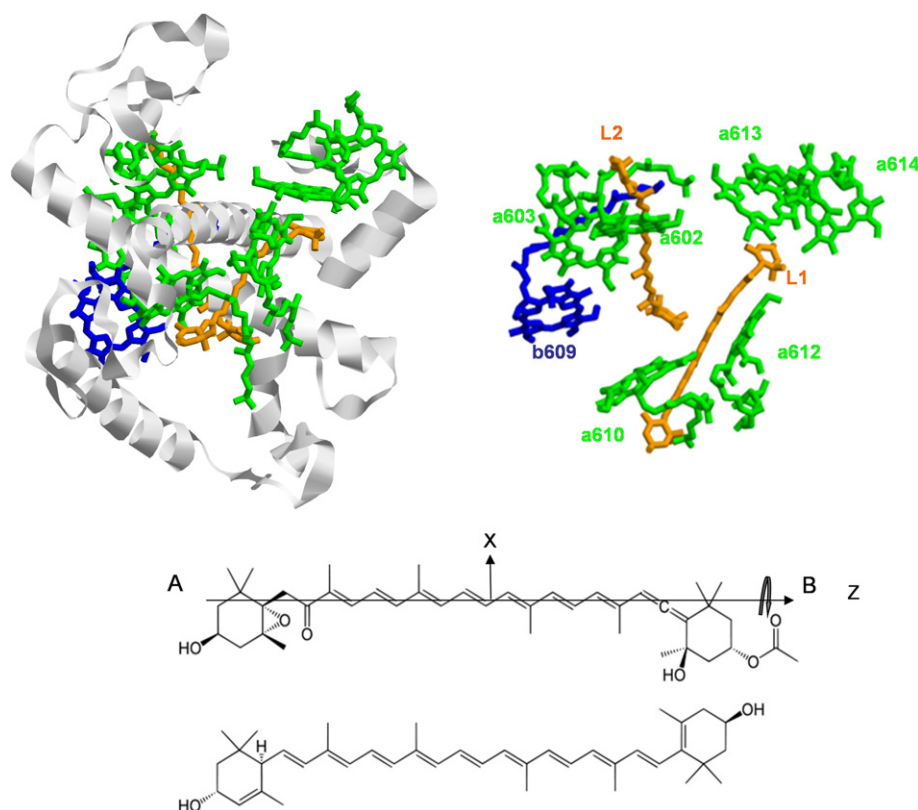

Fig. 1. Top left: structure associated with the core basic unit of the LHCII complex (derived from PDB ID: 1RWT) which corresponds to conserved binding sites in FCP; protein backbone (gray), Chl *b* (blue), Chl *a* (green), and luteins in L1 and L2 sites (orange). Top right: putatively conserved pigments. Bottom: molecular structure schemes of fucoxanthin and lutein. End-groups **A** and **B** are indicated for Fx. Directions of Z and X ZFS axes are also indicated. Clockwise rotations around Z are taken as positive. For all configurations, a reference versus in the Z axis is taken pointing toward the luminal side.

In contrast to LHCII, which binds 14 Chls and 4 Cars [14], FCP binds more Cars and fewer Chls. Different stoichiometries have been proposed up to now, ranging from a 4:4:1 to a 8:8:2 Fx/Chl-*a*/Chl-*c2* per monomer [15,16]. Although this last estimation brings the number of pigments in FCP and LHCII to be the same, most of the Chl *b* molecules are replaced by Fxs [15,16] and the absence of a red-shifted Q*y* band and excitonic signals in the Chl *a*-absorbing region of the circular dichroic spectrum seems to indicate that the FCP pigments have limited close interactions. FCP collects the incident light energy and transfers it to PS I and II [17]. It has been found that, upon excitation of Fx molecules, a significant amount of excitation energy is transferred rapidly to Chl *a* [18]. The lack of spectral evolution in the Chl *a* bleaching band in time resolved absorption spectra, and the fact that it appears at 670 nm [18,19], suggests that the chlorophylls in the FCP complex are not excitonically coupled. Moreover, the fluorescence-excitation measurements indicate that the energy transfer from Chl *c* to Chl *a* is 100% efficient, while not all Fxs in the complex are equally efficient in energy transfer to Chls [18].

A structural model for FCP, based on six Chl *a* plus one Chl *b* conserved ligands and two central carotenoids binding sites as in LHCII, is proposed. This conserved core of pigments is shown in Fig. 1. The position of the extra pigments remains completely unknown even though, based on Raman experiments, a larger number of conserved Chl positions have been suggested [16].

The central luteins of the core of LHCII, bound in L1 and L2 sites, are known to be involved in triplet–triplet energy transfer (TTET) [20]. In this photoprotection process Cars are efficient, fast, and direct quenchers of the Chl *a* triplet states (^{T}Chl) thus preventing the formation of singlet oxygen ($^1O_2^*$) and subsequent harmful oxidation of membrane and protein elements [21]. In our recent Optically Detected Magnetic Resonance (ODMR) study on the triplet states populated under illumination in FCP from *C. meneghiniana*, evidence for the quenching of ^{T}Chl states by Fx

was provided, showing that this Car is indeed able to perform the photoprotective role. ODMR data have shown that two slightly different Car triplet state (^{T}Car) populations are produced which have been assigned to the Cars located in the analogous of L1 and L2 sites of the LHCII structure. However, it was also pointed out that the differences in the interactions among pigments, as revealed by the triplet-minus-singlet spectra of the ^{T}Car states, suggest a different geometry of the Car–Chl pairs involved in TTET in the two light harvesting complexes [22].

In the past, we have studied the formation of ^{T}Car in LHCII from higher plants and in PCP and LHC complexes from dinoflagellates, by means of advanced EPR techniques (Time Resolved EPR, pulse EPR and pulse ENDOR) [23–26]. In LHCII chlorophylls Cla612 and Cla603 (nomenclature as reported in [14]) were identified as the sites having the highest probability of the triplet formation and undergoing triplet quenching by the two central luteins (Lut620 and Lut621). In PCP, Per614 (nomenclature as reported in [27]) has been identified as the specific peridinin playing the main role in the photoprotection mechanism.

In this work we extend our previous ODMR study on the ^{T}Car populated under continuous illumination in isolated FCP, by means of time-resolved (TR-) and pulsed EPR techniques, integrated with quantum mechanical (QM) calculation methods. Starting from the sequence homology of FCP and LHCII, TTET is exploited to gain structural information on the complex in terms of Car–Chl pairs involved in the photoprotective mechanism.

2. Materials and methods

2.1. Sample preparation

FCP complexes from *C. meneghiniana* were prepared according to the method described in [5]. In brief, thylakoids were solubilised

with β-dodecyl maltoside and complexes were separated by sucrose gradient centrifugation. The lower brown band was harvested and concentrated to an OD of 0.85 (1 mm) at 440 nm. The samples used for measurements represented a mixture of FCPa and FCPb complexes, thus having the same pigment composition as the complexes described in [18]. For all the experiments, the FCP samples were dissolved in buffer (6% sucrose, 10 mM Mes pH 6.5, 2 mM KCl, glycerol (60%v/v)).

2.2. Time Resolved EPR

TR-EPR spectra were recorded using a Bruker ER200D X-band spectrometer with an extended detection bandwidth (6 MHz), disabled magnetic field modulation and using pulsed sample photoexcitation from the second harmonic of an Nd:YAG pulsed laser (Quantel Brilliant, λ = 532 nm, pulse length = 5 ns; E/pulse ≅ 5 mJ, 20 Hz repetition rate). The EPR signal was digitized with a LeCroy LT344 digital oscilloscope, triggered by the laser pulse. The overall response time of the instrument was about 150 ns. At each magnetic field position, an average of 100 transient signals was usually recorded. Sample temperature in the range 20 K–300 K was controlled with a helium flow system with 0.5 K accuracy.

2.3. EPR spectral simulations

Simulations of the powder spin-polarised triplet spectra were performed using a program written in Matlab® exploiting the EasySpin routine (ver. 4.5) [28]. The program is based on the full diagonalization of the triplet state spin Hamiltonian, taking into account the Zeeman and magnetic dipole–dipole interactions, assuming a random of molecular orientations with respect to the magnetic field direction. Input parameters are the sublevel populations, the zero field splitting (ZFS) parameters, the line width at the canonical orientations and the g-tensor components.

Calculations of the sublevel triplet state populations of the acceptor (Car), starting from those of the donor (Chl), were performed as before for the LHCII, LHC and PCP complexes [23–26] using a home-written program in Matlab® software, following the formalism of [29], and utilizing the X-ray coordinates of the LHCII protein core. The directions of the ZFS axes of the carotenoid triplet state were obtained applying the procedure of principal component analysis, using the Matlab® function "princomp", as previously described, by considering all the carbon atoms belonging to the conjugated chain [25,26]. The solution vector with the greatest eigenvalue lies (approximately) along the main axis (Z) of the Fx molecule, the vector with the intermediate eigenvalue lies (approximately) along the C–H bonds (X) and the vector with the smallest eigenvalue is perpendicular to the molecular plane (see Fig. 1 for a schematic view).

The program for the calculation of the triplet sublevel populations works in the limit of the high field approximation and in the limit of a TTET process which is fast compared to the time evolution of the donor triplet spectrum (which for ^{T}Chls requires hundred of ns, from 30 K up to 200 K) but slow enough to allow spin alignment in the external magnetic field (this takes places in the picosecond time scale).

2.4. QM/QM calculations

Since the arrangement of the pigments in the FCP complex is not known, we started from the hypothesis of a structural homology between FCP and LHCII [16], and defined a procedure to estimate the compatibility of the possible conformations suggested by the simulation of the triplet EPR spectra, with the arrangement of Fx molecules into the L1 and L2 sites. These sites were previously recognized as the loci of ^{T}Chl quenching in LHCII [21].

The core of FCP was assumed to adopt the polypeptide backbone structure of the core of monomeric LHCII derived from the X-ray

structure (PDB ID: 1RWT) [14]. The positions of Cla602, Cla603, Cla610, Cla612, Cla613 and Cla614, surrounding the central luteins were also conserved. According to the sequence alignment between the spinach LHCII and the FCP from C. meneghiniana [16] many residues facing the carotenoid L2 binding site within 4 Å are non-conserved in FCP. Since the residues facing the carotenoid L1 binding site are mostly conserved, we focussed on the L1 site and changed those few residues which were not conserved, namely Leu172 and Ser190 which in FCP correspond to Lys and Ala respectively, while assuming that the pigment arrangement in the L2 site is similar and symmetric, in terms of relative pigment arrangement to the L1 one, as in LHCII.

A two-layer QM/QM approach [30] was set up for geometry optimization as implemented in the Gaussian software [31]. The inner layer was described using DFT (Density Functional Theory) [32–34]; PBE0 functional [35–37] and 6–31G(d) basis set [38] were employed. This level of theory has been satisfactorily used before for similar systems [39]. The inner layer includes Fx in L1, Cla612 without phytol chain and the asparagine coordinating Cla612.

PM3 Hamiltonian [40,41] was used for the outer layer, which is formed by the pigments and the residues located within 4 Å from the Cla612 and Fx of the inner layer. The backbones of the amino acids belonging to the α-helixes 1 and 3 were frozen during the geometry optimization.

Different initial structures have been considered: 1) Fx has been manually inserted in the same configuration of lutein in the L1 site of LHCII (0°, i.e. identical orientation of the central isoprenoid chain of the Car) and 2) Fx has been inserted as in 1) and rotated of specific angles about its long Z axis (40°, −60°, −140°, 120°: see caption of Fig. 1 for the definition of angle rotation). These angles were selected on the basis of the EPR data as described in the Results section. Since Fx is an asymmetric carotenoid, having two different terminal substituted rings, initial geometries with both directions of insertion have been considered and are denoted "orientation A" and "orientation B", in which the epoxide end group of Fx (see Fig. 1) points toward the lumenal and stromal sides respectively. Since the two ends of Fx have different steric hindrance, the definition of the outer layer is different (different residues) for A and B. The residues whose backbones are kept frozen are also different for A and B, namely Met73, Ala76, Leu77, Gly78, Cys79, Val80, Leu176, Lys179, Asn183, Leu186, Ala187, Ser190, Gly193, Phe 194, Gln197 for A; Ala72, Met73, Leu74, Ala76, Leu77, Val80, Leu84, Leu176, Lys179, Asn183, Gly184, Leu186, Ala187, Met188, Phe189, Ser190, Met191, Gly193, Phe194, and Gln197 for B (note that all residues are numbered according to LHCII sequence). Additionally, in B, because of a steric interaction between Ser190 and Fx, the former was included in the inner layer.

3. Results

3.1. TR-EPR

Continuous illumination of isolated FCP complexes at cryogenic temperatures leads to the formation of ^{T}Car as previously revealed by ODMR spectroscopy [22]. Two different ^{T}Car populations were detected by ODMR: T1 (with ZFS parameters: |D| = 45.1 mT, |E| = 4.35 mT) and T2 (|D| = 46.6 mT, |E| = 4.35 mT). Since it is known that ^{T}Cars are not populated directly from the excited singlet states [21], their presence in the antenna complexes was attributed to ^{T}Chl quenching. Illumination of the complex at 1.8 K resulted also in the production of ^{T}Chls which were not quenched by the carotenoids, having ZFS parameters: |D| = 30.5–30.8 mT and |E| = 4.21 mT. These triplets were assigned to the "red most" chlorophylls of the complex, on the basis of their microwave-detected triplet-minus-singlet spectra [22]. No Chl c triplet states were detected [22].

The triplet states revealed by ODMR can also be detected by pulsed laser illumination of the samples in conjunction with time-resolved or

pulse EPR detection. Fig. 2 shows the 30 and 200 K X-band spin-polarized TR-EPR spectra of FCP, taken 150 ns after the laser pulse. The spectra reveal the presence of, at least, two different species. The prevalent triplet, having ZFS parameters: |D| = 30.0 ± 0.5 mT and |E| = 3.8 ± 0.01 mT, can be easily assigned to [T]Chl *a*, on the basis of the ZFS parameters determined by ODMR spectroscopy reported above, and by comparison with the well-known in vitro TR-EPR spectrum of [T]Chl *a* [25].

The presence of [T]Car in the composite spectrum is revealed by the transitions corresponding to the canonical orientation Z (separated by 2|D|, |D| = 46.3 mT), which do not overlap with the transitions due to [T]Chl *a*. The observed |D| parameter is close to the values of the |D| parameters determined by ODMR even though two different carotenoid triplet states cannot be resolved. The relatively large contribution of [T]Chl *a*, to the TR-EPR spectrum, is partially reduced at higher temperature (Fig. 2).

Two-pulse ESE experiments have been successfully used before for the analysis of the EPR spectra of the photo-induced triplet states in LHCII, LHC and PCP [23–26]. In those cases the shape of TR-EPR and ESE detected spectra of [T]Cars, taken at short delay after the laser flash, the same as in this work, i.e. 150 ns, was identical, due to the absence of fast and anisotropic relaxation processes, at the temperature of the experiments (30 K). In contrast, the ESE detected spectrum of FCP shows the absence of the Z components, making it difficult to exploit the remaining features to extract the "pure" contribution of the [T]Car states (Fig. S1 Supplementary data). Nevertheless, by taking the difference between the two TR-EPR spectra taken at 30 and 200 K, which contain a different relative contribution of [T]Chl *a*, after normalization of the intensity of the spectra on the Z transitions of the carotenoids, the pure spectrum of [T]Chl *a* can be obtained. As a consequence the whole spectrum may be reconstructed into its components and the pure [T]Car spectrum obtained as well, see Fig. 2 (the parameters used in the spectra reconstruction are reported in Table 1). The spin polarization of the [T]Car component determined from this reconstruction of the spectrum is: *eeeaaa* (*a* stands for absorption and *e* for emission). Compared to the polarization pattern observed in LHCII from higher plants and LHC from dinoflagellates, i.e. *eeaeaa*, the FCP complex presents reversed central lines. Since [T]Car inherits the

Table 1
Parameters[a] of triplet state simulations for the reconstruction of TR-EPR spectra reported in Fig. 2.

	[T]Chl *a*	[T]Fx
30 K		
|D| [mT]	30.1 ± 0.05	46.3 ± 0.05
|E| [mT]	4.1 ± 0.05	4.2 ± 0.05
$P_x:P_y:P_z$	0.37:0.41:0.22	0.22:0.30:0.48
$W_x:W_y:W_z$ [mT]	2.0:1.5:2.5	2.8:1.5:2.0
g_x,g_y,g_z	2.0023	2.0023
Relative amplitude	3.45	1
200 K		
|D| [mT]	30.0 ± 0.05	46.3 ± 0.05
|E| [mT]	3.8 ± 0.05	4.4 ± 0.05
$P_x:P_y:P_z$	0.37:0.41:0.22	0.22:0.30:0.48
$W_x:W_y:W_z$ [mT]	2.0 ± 0.1:2.5 ± 0.1:2.0 ± 0.1	3.7 ± 0.1:2.0 ± 0.1:2.0 ± 0.1
g_x,g_y,g_z	2.0023	2.0023
Relative amplitude	1.45	1

[a] $P_x:P_y:P_z$, zero field populations of the triplet state sublevels of Chl *a* and Fx triplet states. |D| and |E|: ZFS parameters. W_i: line width at the canonical positions in the EPR powder spectrum, g_i: principal values of g-tensor.

polarization pattern from [T]Chl *a*, this means that a different relative configuration between the Chl and Car pairs involved in TTET has been adopted in this complex.

The time evolution of the spin polarization was investigated by monitoring the TR-EPR spectrum at different delay times (see Fig. 3). The Z component has a decay time of about 8 μs while the polarization of the Y component is inverted after about 6 μs. These effects are expected on the basis of the anisotropy of the decay rates of the spin sublevels, as previously reported for the kinetics of [T]Car in other systems [26,29,42], and have contributed to the correct reconstruction of the spectrum at initial time. The spectrum detected at long times after the laser flash allows a more precise determination of the X and Y canonical transition field positions of the [T]Car state, because of the reduced contribution of the [T]Chl component. The time evolution of the [T]Car spectrum is slow compared to the time scale of the TTET, thus the spectra taken at the earliest time reflect the "initial" polarization inherited from the [T]Chls. The Chl contribution to the TR-EPR spectrum evolves independently showing no correlation with the time evolution of the [T]Car, meaning that it is due to [T]Chls which are not quenched by Cars and hence are unprotected Chls.

3.2. EPR spectral analysis and computational results

In analogy with other light harvesting complexes, the formation of [T]Car in FCP is thought to arise from [T]Chl *a* quenching. The spin polarized
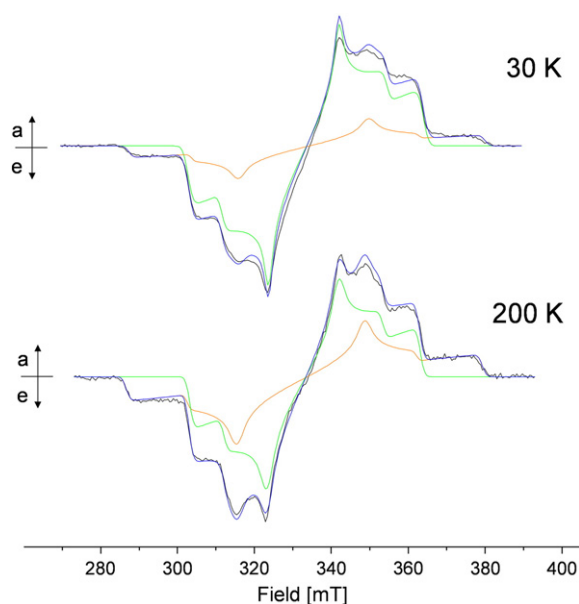

Fig. 2. X-band spin-polarized TR-EPR spectra of the photoexcited triplet states populated in FCP at 30 and 200 K as indicated (black solid lines); delay after the laser flash: 150 ns. (a = absorption, e = emission). Reconstructions (blue) of the TR-EPR spectra obtained by summing the [T]Chl *a* contribution (green line) and the [T]Car contribution (orange line). Simulation parameters are reported in Table 1.
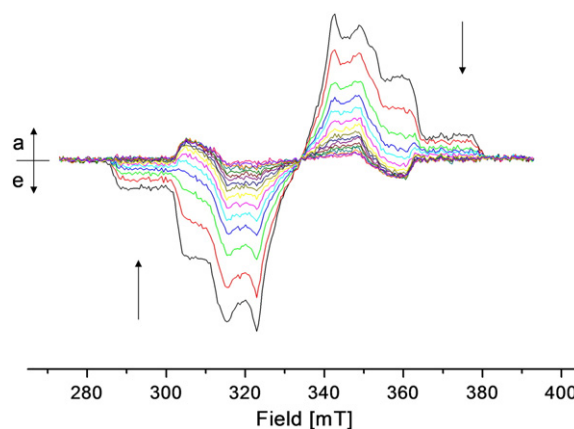

Fig. 3. X-band spin-polarized TR-EPR spectra of FCP at different delay times after the laser flash (traces from 0.5 to 15.5 μs with 1 μs step). T = 200 K. Arrows indicate the time progression. (a = enhanced absorption, e = enhanced emission).

spectrum of ^{T}Car conserves the polarization pattern inherited from the ^{T}Chl donor, due to the occurrence of spin conservation during TTET. We have already discussed in details this point in our previous work on PCP, LHC and LHCII [43,25,26] and have shown that the pairs involved in TTET can be identified by comparing the spin polarization derived from the experimental TR-EPR spectrum with that calculated on the basis of the structure of the complex and the orientation of the ZFS axes on the pigment molecular frames.

Although the structure of FCP is not available, the sequence alignment allows the hypothesis of a structural similarity with the LHCII complex, as in the case of LHC [25]. In particular the structure of the *core* of the protein, composed by the central Cars, which are the sites of ^{T}Chl *a* quenching in LHCII, and chlorophylls Cla610–612–602–603–613–614, is expected to be conserved (Fig. 1) [16]. By assuming a conserved relative geometry of carotenoids and Chls in the core of the complex, the parameters to be set for the calculations of the Car spin polarized triplet spectrum are: 1) the values of the ZFS parameters; 2) the directions of the ZFS axes in relation to the molecular frame, for both the donor (Chl) and the acceptor (Fx); and 3) the sublevel population rates of the ^{T}Chl *a*.

The ^{T}Chl *a* ZFS axes used are those previously defined for ^{T}Chl *a* in LHCII [26], while the ZFS axes of the inserted Fx have been obtained by the procedure used for the PCP complex, as described in the Materials and methods section. In fact, differently to what is observed for singlet states, calculations of the electronic distribution of the peridinin triplet state, based on experimental ENDOR data on PCP, have shown that the triplet state maintains the same characteristics of lutein in LHCII, meaning that it is mainly determined by the long conjugated chain [23] rather than by the substituents. Since the molecular structure of Fx is similar to that of peridinin, it seems reasonable that the ZFS directions are properly determined by the same method used for peridinin in PCP.

Due to the fast TTET, the spectral features of the ^{T}Chl *a* states, which are specifically quenched by the carotenoids in FCP, cannot be identified. Consequently, we have to also make some assumptions in terms of the sublevel populations of the ^{T}Chl *a*, to be projected from the donor to the acceptor triplet in order to calculate the ^{T}Car acceptor populations. As in our previous work [25,26], we present the calculations for the population rates of the acceptor triplet obtained by using the ^{T}Chl *a* populations which produce the *eeeaaa* spectral pattern observed also for the unquenched ^{T}Chl *a* states in FCP (Fig. 2, green line).

We have calculated the initial ^{T}Car spectra, expected on the basis of the TTET mechanism, for all the Cla610–612–613–614/Fx mutual configurations derived from LHCII structure after substitution of luteins with Fxs (Fig. 4). (The overall set of parameters used for the calculations can be found in the Supplementary data). Note that Cla602 and Cla603 give equivalent spectra to Cla610 and Cla612. Although the structure of the Fx in the L1/L2 sites has not been optimized for this evaluation, the calculations demonstrate that none of the Chls of the core shows the polarization pattern of the experimental EPR spectrum. Thus, in the hypothesis of a general structural similarity between the LHCII and the FCP and in the hypothesis of a conserved photoprotective function of Cars located in the L1/L2 sites, a local molecular rearrangement of the carotenoid/chlorophyll molecules must be considered. This rearrangement might be due to the different molecular structures of Fx compared to that of lutein.
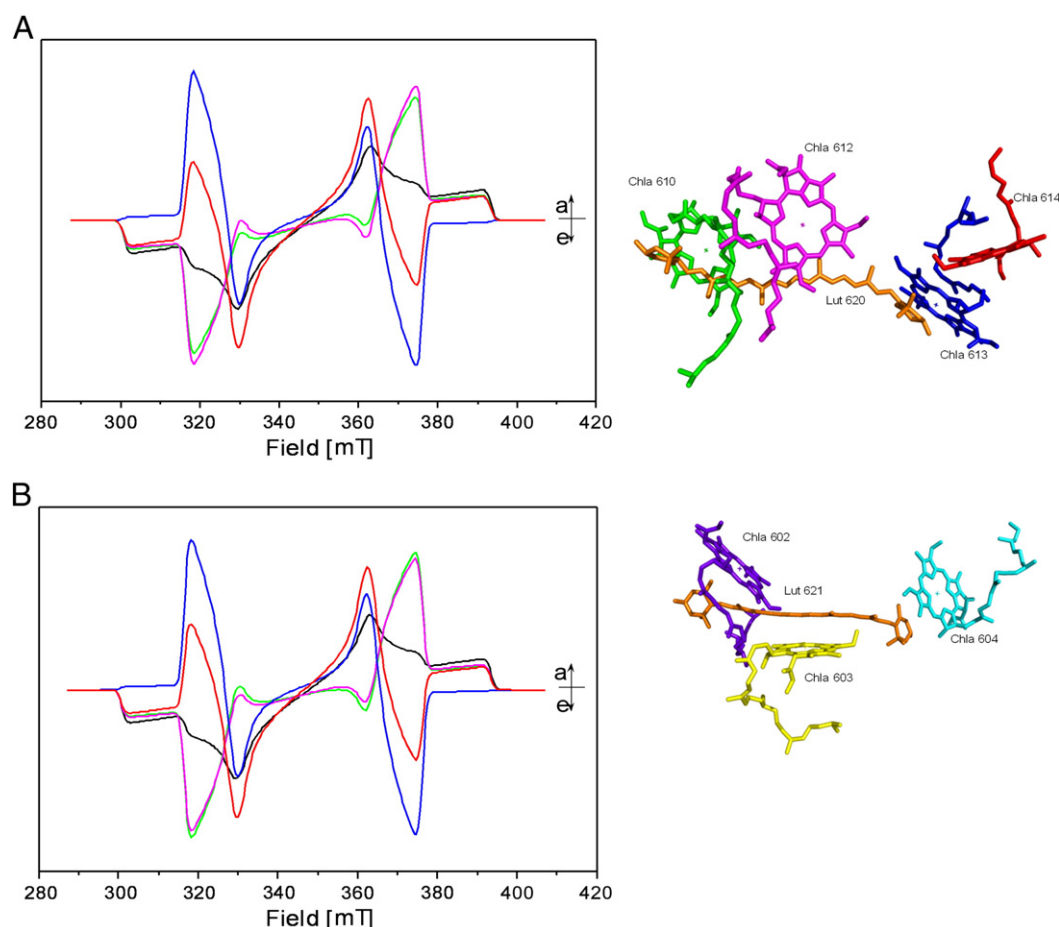

Fig. 4. ^{T}Fx TR-EPR spectrum in L1 site of LHCII populated via TTET starting from conserved Chls. Experimental spectrum is shown in black. Color code according to the reported molecular structure of L1 and L2 sites of triplet quenching in LHCII; Chls *a* conserved in FCP are shown together with luteins 620/621 (orange).
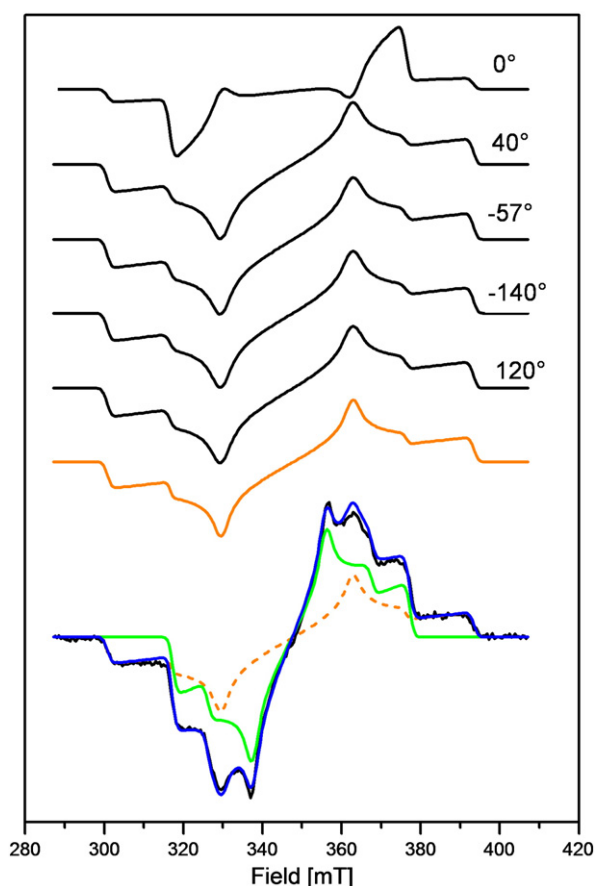
Fig. 5. Fx triplet state spectra calculated by TTET starting from ^{T}Cla612 (|D|,|E| = 30.1, 4.1 mT; P_x:P_y:P_z = 0.37:0.41:0.22; W_x:W_y:W_z [mT] = 2.0:1.5:2.5; g = 2.0023) after rotation of Fx along its Z-axis in L1 site, as indicated. Only angles which correspond to geometries able to reproduce the experimental spectrum (orange) are shown.

Based on the assumption that the chlorophyll triplets quenched by Cars are those formed in Cla603/Cla612 as in LHCII, and on the basis of the cylindrical shape of the protein pocket where the Cars are located

we consider that the most likely rearrangement to occur is a rotation of the carotenoid around its long symmetry axis. The calculation of TTET from Cla603/Cla612 shows that the experimental ^{T}Car EPR spectrum can be reproduced for a limited number of rotation angles, namely 40°, −57°, −140°, and 120° (see Fig. 5).

To estimate if some of the conformations that give rise to TR-EPR spectra compatible with those observed correspond to plausible structures of the protein *core* of FCP, multi-layer QM calculations have been performed. Optimization of the core structure was performed starting from different initial configurations prepared by inserting the Fx in the L1 site in the same configuration of the lutein (0°) and rotating Fx about its long ZFS axis by the four different angles (40°, −57°, −140°, 120°) that gave rise to acceptable simulations of EPR spectra. In addition, due to the asymmetry of the carotenoid, both directions of insertion of Fx have been considered, denoted orientation **A** and orientation **B**, for a total of ten initial structures (note that rotation angles are given with respect to the Z-axis before inversion of the carotenoid in the site, which correspond to a further 180° rotation of the Fx with respect to the X-axis). The results obtained for some significant conformations are reported in Fig. 6, where the Cla612-Fx pairs are shown as input and output structures. During the geometry optimizations Fx rotated about its long axis from the initial (input) position. In some cases the optimized structures were characterized by strong distortion of the Fx conjugated chain and for this reason have been discarded (data not shown). Among all the optimized geometries, only that obtained starting from a −140° rotation angle (in orientation **B**) leads to a calculated ^{T}Car spectrum compatible with the experimental one, in terms of polarization pattern (Fig. 7). In the optimized configuration Fx is rotated of about −120° and also slightly tilted while Cla612 undergoes a small shift with respect to the crystal structure. In Fig. 7 a comparison between this optimized core structure of FCP and that of LHCII is shown.

4. Discussion

The EPR results obtained for FCP show that the TTET between Chl and Fx is active up to 200 K but, despite the high Car/Chl ratio, the efficiency of the quenching of ^{T}Chl *a* is low. In fact a population of unquenched ^{T}Chl *a* is present, which is even larger than that observed before in LHC and LHCII [24,25] as revealed also by ODMR [22].
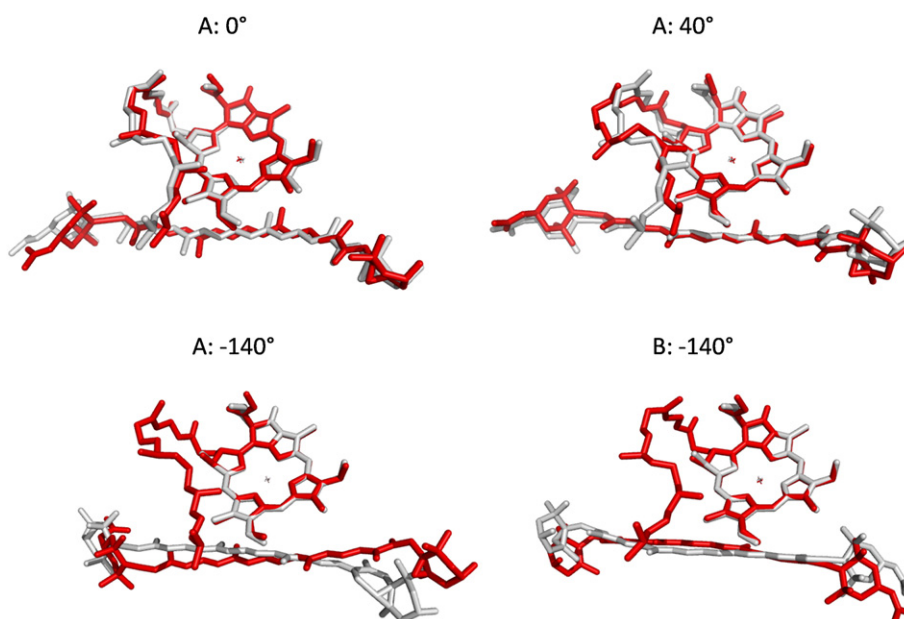

Fig. 6. Some significant conformations of Fx/Cla612 obtained after optimization (red) of the core structure starting from different initial configurations (gray) as indicated: insertion of the Fx molecule in the same configuration of lutein in the L1 site of LHCII (**A**: 0°); insertion of Fx after rotation along its long Z axis (**A**: 40°; **A**: −140°; **B**: −140°).
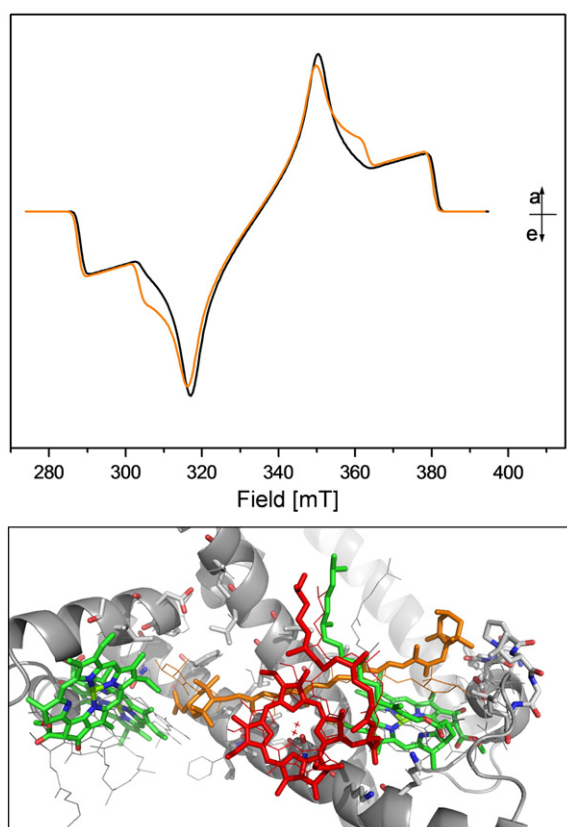
Fig. 7. Top: 30 K TR-EPR spectrum of ^{T}Fx component (orange), also reported in Fig. 2, and TR-EPR spectrum of ^{T}Fx calculated on the basis of TTET from ^{T}Cla612 (black). Fx/Cla612 structures as derived from optimized conformation **B**: −140°. Parameters for donor ^{T}Chl as in [22]; calculated ^{T}Fx populations Px:Py:Pz = 0.29:0.33:0.38; other parameters as in Table 1. Bottom: comparison between the optimized conformation (**B**: −140°) of FCP core (thick) and the structure of LHCII (thin). Color code: Fx (orange), Cla612 (red), other Chls (green for FCP and gray for LHCII). Non-conserved amino acids are highlighted.

The proposed structural model for FCP based on six Chl *a* plus one Chl *b* conserved ligands and on two conserved central binding sites for Cars suggests that, also in FCP as in LHCII, the L1 and L2 sites may well be the sites of ^{T}Chl quenching. However, as we have discussed in our previous ODMR work, the absence of the bleaching of Chl *c* in the triplet minus singlet spectra associated to ^{T}Car states in FCP clearly indicates that Chl *b* is not just replaced by Chl *c* in the FCP protein structure [22]. Moreover Cla611, which is coordinated by a phospholipid in LHCII, is likely to be absent in FCP [16]. Thus, the altered molecular composition of the site, where an asymmetric carotenoid like Fx substitutes the lutein molecule, and the change in the interactions among pigments, and in particular the absence of Chl *b*, may be responsible for the observed difference in the relative geometry of the Car–Chl pairs involved in TTET, as revealed by the EPR experiments. The spectral analysis reported in [26] has shown that the initial polarization pattern of the ^{T}Car detected in LHCII by TR-EPR and pulse EPR may be reproduced by considering a single TTET step from Cla603 to Lut621 (site L2) and/or from Cla612 to Lut620 (site L1). The largely varied spin polarization of the ^{T}Car states observed for FCP here points toward a different pigment organization of the central carotenoids and surrounding Chls compared to LHCII.

On the basis of the calculations reported in the Results section, some conclusions can be drawn. If the similarity with LHCII extends at the level of the Chl/Car pairs involved in TTET (namely L1, L2 and Cla603/612), then the Fx/Chl molecules are oriented relative to each other in a different way, compared to the lutein/Chl pairs. This is probably a consequence of the different structures of the two end groups of Fx and the absence of Chl *b*/Chl *a* interactions, which affects the site energies in the core of FCP.

As suggested by the comparison between the experimental EPR spectrum and QM results, the most likely rearrangement of the photoprotective site corresponds roughly to a −120° rotation of Fx about its long axis (Euler angles are reported in Table S3 Supplementary data). This may have a consequence on the loss of Chl triplet quenching, when compared to that of LHCII, and could explain the large amount of observed unquenched ^{T}Chl states populated upon illumination. In fact, a different relative arrangement of Fx–Chl *a* pairs compared to Lut–Chl *a* pairs in LHCII, together with a change on Chl–Chl interactions due to the absence of Cla611 and Chl *b*, may lead to a different excitation energy distribution among the Chls close to L1 and L2 sites, because of the change in the local site energies. It may be worth noting that during the QM geometry optimization starting from different angles, Fx rotates with respect to its initial position about its long ZFS Z axis; and in some cases Fx bends anomalously loosing conjugation. In geometries with orientation **B** we have noticed that the steric hindrance at the end of Fx pointing on the stromal side induces the Fx to escape from the cavity where it has been inserted. This translation of the carotenoid is accompanied by strong deformations which occur to accommodate the imposed constraints. When such severe distortions occurred, also in the geometries with orientation **A**, the resulting optimized core structures were discarded due to their poor physical meaning. Among the suitable geometries with orientation **A** the lowest energy structure is obtained starting from a Z-axis rotation of −140°, while starting from 0° and 40° the calculations converged to minima with very similar but higher energies. Among the geometries with orientation **B** the lowest energy structure is obtained starting from −140°. The computed spectrum based on the corresponding output structure is the only one, among all the calculated structures, which is in reasonable agreement with the experimental spectrum. It is important to note that starting from the lutein-like 0° orientation, Fx is found slightly rotated but significantly translated and distorted in the converged minimum energy final structure. Thus, both the configurations in which the Fx is inserted in the protein core as lutein (°0) do not represent an energy minimum; conversely, some of the rotated structures seem to be more stable (see Table S2 in Supplementary data).

An alternative explanation for the EPR results could be the direct involvement in the TTET process of other Fxs present in each FCP monomer besides the ones in L1 and L2. In that case, due to the lack of structural information on the protein constrains, the exact orientation of the Chl/Car pairs involved in TTET cannot be inferred. In fact the number of relative geometries which could give rise to the observed polarization pattern in the TR-EPR spectrum of ^{T}Fx, within the experimental uncertainty, is very large (the details of the general method used to determine all the possible configurations which produce a given polarization pattern will be published elsewhere). Therefore, in this case it would be impossible to give a univocal geometry of the pairs involved in the photoprotective mechanism of ^{T}Chl quenching. However, on the basis of our previous ODMR results, which have shown an extended spectral similarity of FCP with the LHCII complex, the specific involvement of the extra fucoxanthins in the direct quenching of chlorophyll triplet states seems to be unlikely.

It may be surprising that a complex which is richer in carotenoids than LHCII presents a higher contribution of unquenched Chl triplet states. However, it is well known that also in LHCII two carotenoids, namely neoxanthin and violaxanthin, are not involved in TTET, and "unquenched" Chls are observed in this complex as well, although in minor amount. There are strict geometrical requirements for TTET in particular close proximity provides the necessary overlap of the wavefunctions of donor and acceptor, thus some carotenoids may not fulfill these conditions relatively to specific Chls present in the protein. It is worth noting that some Fxs are not involved even in singlet energy transfer to Chls [18] suggesting that they may have a role similar to that of neoxanthin in LHCII, consisting in the direct quenching of singlet oxygen. As suggested in [15], the bluer Fxs,

which are less efficient at energy transfer to Chl *a*, may be involved in transferring their absorbed energy to the red Fxs.

5. Conclusions

This study on the quenching mechanism of ^{T}Chl in isolated FCP complex from *C. meneghiniana* confirms the suggestion of our previous work on FCP, which revealed a local different arrangement of the pigments involved in the photoprotective mechanism, compared to the structure of the photoprotective sites of LHCII. Indeed, the TR-EPR experiment has revealed a variation on the spin polarization pattern of the triplet state spectrum of Fx, which is indicative of a variation of the relative configuration of the Chl–Car pair involved in the photoprotection.

We suggest a model for the interpretation of the spectroscopic data, based on the analogy with the "core" of LHCII. In the assumption of a conserved function of carotenoids in L1–L2 sites, a putative conformation described by a rotation of the carotenoid Fx in the L1 site of about −120° along its long axis has been calculated.

It is worth noting that in principle, other Fx–Chl *a* pairs, together with those belonging to the L1 and L2 sites, could contribute to the observed ^{T}Car TR-EPR spectrum. However, in general, different geometries of the Chl–Car pairs would lead to a decrease of the intensity of the whole spectrum, because of different signs of the polarization patterns. Thus it seems unlikely that many different Fxs contribute to the observed spectrum. Moreover, in the ODMR spectra, which are more sensitive to the influence of different protein environments on the ZFS parameters, there was no evidence of the presence of more than two ^{T}Cars [22].

Although, due to the large number of assumptions which have necessarily been adopted for the calculations of the TR-EPR spectrum, the assignment of the Chl–Car pairs involved in TTET in the conserved core remains speculative, nevertheless a local rearrangement of the Car–Chl *a* pairs in the L1 and L2 sites, compared to that present in LHCII, as suggested by QQ/QM calculations, is likely to occur, because of the steric effect of the Fx terminal rings and of the absence of close interactions among chlorophylls in the site.

Acknowledgements

Appendix A. Supplementary data

Supplementary data to this article can be found online at http://dx.doi.org/10.1016/j.bbabio.2013.07.003.

References

[1] A.M. Pyszniak, S.P. Gibbs, Immunocytochemical localization of photosystem I and the fucoxanthin-chlorophyll a/c light-harvesting complex in the diatom *Phaeodactylum tricornutum*, Protoplasma 166 (1992) 208–217.

[2] B. Grrabowski, F.X. Cunningham, E. Gantt, Chlorophyll and carotenoid binding in a simple red algal light-harvesting complex crosses phylogenetic lines, Proc. Natl. Acad. Sci. 98 (2001) 2911–2916.

[3] E. Pichersky, B.R. Green, The extended family of chlorophyll *a/b*-binding proteins of PS I and PS II, in: M. Baltscheffsky (Ed.), Current Research in Photosynthesis, Vol 3, Kluwer Academic publishers, Dordrecht, the Netherlands, 1990, pp. 553–556.

[4] A. De Martino, D. Douady, M. Quinet-Szely, B. Rousseau, F. Crepineau, K. Apt, L. Caron, The light-harvesting sntenna of brown algae, Eur. J. Biochem. 267 (2000) 5540–5549.

[5] C. Büchel, Fucoxanthin-chlorophyll proteins in diatoms: 18 and 19 kDa subunits assemble into different oligomeric states, Biochemistry 42 (2003) 13027–13034.

[6] A. Beer, K. Gundermann, J. Beckmann, C. Büchel, Subunit composition and pigmentation of fucoxanthin-chlorophyll proteins in diatoms: evidence for a subunit involved in diadinoxanthin and diatoxanthin binding, Biochemistry 45 (2006) 13046–13053.

[7] J. Lavaud, B. Rousseau, A.L. Etienne, Enrichment of the light-harvesting complex in diadinoxanthin and implications for the non-photochemical fluorescence quenching in diatoms, Biochemistry 42 (2003) 5802–5808.

[8] G. Guglielmi, J. Lavaud, B. Rousseau, A.L. Etienne, J. Houmard, A.V. Ruban, The light-harvesting antenna of the diatom *Phaeodactylum tricornutum*. Evidence for a diadinoxanthin-binding subcomplex, FEBS Lett. 272 (2005) 4339–4348.

[9] K. Gundermann, C. Büchel, The fluorescence yield of the trimeric fucoxanthin chlorophyll–protein FCPa in the diatom *Cyclotella meneghiniana* is dependent on the amount of bound diatoxanthin, Photosynth. Res. 95 (2008) 229–235.

[10] R. Goss, T. Jakob, Regulation and function of xanthophyll cycle-dependent photoprotection in algae, Photosynth. Res. 106 (2010) 103–122.

[11] B.R. Green, E. Pichersky, Hypothesis for the evolution of three-helix Chl a/b and Chl a/c light-harvesting antenna proteins from two-helix and four-helix ancestors, Photosynth. Res. 39 (1994) 149–162.

[12] G.R. Wolfe, F.X. Cunningham, D. Durnford, B.R. Green, E. Gantt, Evidence for a common origin of chloroplasts with light-harvesting complexes of different pigmentation, Nature 367 (1994) 566–568.

[13] D.G. Durnford, R. Aebersold, B.R. Green, The fucoxanthin-chlorophyll proteins from a chromophyte alga are part of a large multigene family: structural and evolutionary relationships to other light-harvesting antennae, Mol. Gen. Genet. 253 (1996) 377–386.

[14] Z. Liu, H. Yan, K. Wang, T. Kuang, J. Zhang, L. Gui, X. An, W. Chang, Crystal structure of spinach major light-harvesting complex at 2.72 Å resolution, Nature 428 (2004) 287–292.

[15] L. Premvardhan, L. Bordes, A. Beer, C. Büchel, B. Robert, Carotenoid structures and environments in trimeric and oligomeric fucoxanthin chlorophyll a/c$_2$ proteins from resonance Raman spectroscopy, J. Phys. Chem. B 113 (2009) 12565–12574.

[16] L. Premvardhan, B. Robert, A. Beer, C. Büchel, Pigment organization in fucoxanthin chlorophyll a/c(2) proteins (FCP) based on resonance Raman spectroscopy and sequence analysis, Biochim. Biophys. Acta Bioenerg. 1797 (2010) 1647–1656.

[17] T. Veith, J. Brauns, W. Weisheit, M. Mittag, C. Büchel, Identification of a specific fucoxanthin-chlorophyll protein in the light harvesting complex of photosystem I in the diatom *Cyclotella meneghiniana*, Biochim. Biophys. Acta Bioenerg. 1787 (2009) 905–912.

[18] E. Papagiannakis, I.H.M. van Stokkum, H. Fey, C. Büchel, R. van Grondelle, Spectroscopic characterization of the excitation energy transfer in the fucoxanthin-chlorophyll protein of diatoms, Photosynth. Res. 86 (2005) 241–250.

[19] N. Gildenhoff, S. Amarie, K. Gundermann, A. Beer, C. Büchel, J. Wachtveitl, Oligomerization and pigmentation dependent excitation energy transfer in fucoxanthin-chlorophyll proteins, Biochim. Biophys. Acta Bioenerg. 1797 (2010) 543–549.

[20] S.S. Lampoura, V. Barzda, G.M. Owen, A.J. Hoff, H. van Amerongen, Aggregation of LHCII leads to a redistribution of the triplets over the central xanthophylls in LHCII, Biochemistry 41 (2002) 9139–9144.

[21] H.A. Frank, R.J. Cogdell, Carotenoids in photosynthesis, Photochem. Photobiol. 63 (1996) 257–264.

[22] M. Di Valentin, C. Büchel, G.M. Giacometti, D. Carbonera, Chlorophyll triplet quenching by fucoxanthin in the fucoxanthin-chlorophyll protein from the diatom *Cyclotella meneghiniana*, Biochem. Biophys. Res. Commun. 427 (2012) 637–641.

[23] E. Salvadori, M. Di Valentin, C.W.M. Kay, A. Pedone, V. Barone, D. Carbonera, The electronic structure of the lutein triplet state in plant light-harvesting complex II, Phys. Chem. Chem. Phys. 14 (2012) 12238–12251.

[24] M. Di Valentin, C. Tait, E. Salvadori, S. Ceola, H. Scheer, R.G. Hiller, D. Carbonera, Conservation of spin polarization during triplet–triplet energy transfer in reconstituted peridinin–chlorophyll–protein complexes, J. Phys. Chem. B 115 (2011) 13371–13380.

[25] M. Di Valentin, E. Salvadori, G. Agostini, F. Biasibetti, S. Ceola, R.G. Hiller, G.M. Giacometti, D. Carbonera, Triplet–triplet energy transfer in the major intrinsic light-harvesting complex of *Amphidinium carterae* as revealed by ODMR and EPR spectroscopies, Biochim. Biophys. Acta Bioenerg. 1797 (2010) 1759–1767.

[26] M. Di Valentin, F. Biasibetti, S. Ceola, D. Carbonera, Identification of the sites of chlorophyll triplet quenching in relation to the structure of LHCII from higher plants. Evidence from EPR spectroscopy, J. Phys. Chem. B 113 (2009) 13071–13078.

[27] E. Hofmann, P.M. Wrench, F.P. Sharples, R.G. Hiller, W. Welte, K. Diederichs, Structural basis of light harvesting by carotenoids: peridinin chlorophyll–protein from *Amphidinium carterae*, Science 272 (1996) 1788–1791.

[28] S. Stoll, A. Schweiger, EasySpin, a comprehensive software package for spectral simulation and analysis in EPR, J. Magn. Reson. 178 (2006) 42–55.

[29] D. Carbonera, M. Di Valentin, C. Corvaja, G. Agostini, G. Giacometti, P.A. Liddel, D. Kuciauskas, A.L. Moore, T.A. Moore, D. Gust, Carotenoid triplet detection by time-resolved EPR spectroscopy in carotenopyropheophorbide dyads, J. Photochem. Photobiol. 105 (1997) 329–335.

[30] S. Dapprich, I. Komáromi, K.S. Byun, K. Morokuma, M.J. Frisch, A new ONIOM implementation in Gaussian 98. 1. The calculation of energies, gradients and vibrational frequencies and electric field derivatives, J. Mol. Struct. (Theochem) 462 (1999) 1–21.

[31] Gaussian 03, Revision B.05. M.J. Frisch, G.W. Trucks, H.B. Schlegel, G.E. Scuseria, M.A. Rob, J.R. Cheeseman, J.A. Montgomery Jr., T. Vreven, K.N. Kudin, J.C. Burant, J.M. Millam, S.S. Iyengar, J. Tomasi, V. Barone, B. Mennucci, M. Cossi, G. Scalmani, N. Rega, G.A. Petersson, H. Nakatsuji, M. Hada, M. Ehara, K. Toyota, R. Fukuda, J. Hasegawa, M. Ishida, T. Nakajima, Y. Honda, O. Kitao, H. Nakai, M. Klene, X. Li, J.E. Knox, H.P. Hratchian, J.B. Cross, V. Bakken, C. Adamo, J. Jaramillo, R. Gomperts, R.E. Stratmann, O. Yazyev, A.J. Austin, R. Cammi, C. Pomelli, J.W. Ochterski, P.Y. Ayala, K. Morokuma, G.A. Voth, P. Salvador, J.J. Dannenberg, V.G. Zakrzewski, S. Dapprich, A.D. Daniels, M.C. Strain, O. Farkas, D.K. Malick, A.D. Rabuck, K. Raghavachari, J.B. Foresman, J.V. Ortiz, Q. Cui, A.G. Baboul, S. Clifford, J. Cioslowski, B.B. Stefanov, G. Liu, A. Liashenko, P. Piskorz, I.

Komaromi, R.L. Martin, D.J. Fox, T. Keith, M.A. Al-Laham, C.Y. Peng, A. Nanayakkara, M. Challacombe, P.M.W. Gill, B. Johnson, W. Chen, M.W. Wong, C. Gonzalez, J.A. Pople, Gaussian 03, Gaussian, Inc., Wallingford, CT, 2004.

[32] P. Hohenberg, W. Kohn, Inhomogeneous electron gas, Phys. Rev. 136 (1964) B864–B871.

[33] W. Kohn, L.J. Sham, Self-consistent equations including exchange and correlation effects, Phys. Rev. 140 (1965) A1133–A1138.

[34] R.G. Parr, W. Yang, Density-functional Theory of Atoms and Molecules, Oxford University Press, New York, 1989.

[35] J.P. Perdew, K. Burke, M. Ernzerhof, Generalized gradient approximation made simple, Phys. Rev. Lett. 77 (1996) 3865–3868.

[36] J.P. Perdew, K. Burke, M. Ernzerhof, Errata: generalized gradient approximation made simple, Phys. Rev. Lett. 78 (1997) 1396–1399.

[37] C. Adamo, V. Barone, Toward reliable density functional methods without adjustable parameters: the PBE0 model, J. Chem. Phys. 110 (1999) 6158–6169.

[38] Basis sets were obtained from the Extensible Computational Chemistry Environment Basis Set Database, Version 02/25/04, as developed and distributed by the Molecular Science Computing Facility, Environmental and Molecular Sciences Laboratory which is part of the Pacific Northwest Laboratory, P. O. Box 999, Richland, Washington 99352,USA, and funded by the U.S. Department of Energy. The Pacific Northwest Laboratory is a multi-program laboratory operated by Battelle Memorial Institute for the U.S. Department of Energy under contract DE-AC06-76RLO 1830.

[39] L. Orian, S. Carlotto, M. Di Valentin, A. Polimeno, Charge transfer in model bioinspired carotene–porphyrin dyads, J. Phys. Chem. A 116 (2012) 3926–3933.

[40] J.J.P. Stewart, Optimization of parameters for semiempirical methods. I. Method, J. Comput. Chem. 10 (1989) 209–220.

[41] J.J.P. Stewart, Optimization of parameters for semiempirical methods. II. Applications, J. Comput. Chem. 10 (1989) 221–264.

[42] R. Bittl, E. Schlodder, I. Geisenheimer, W. Lubitz, R.J. Cogdell, EPR and absorption studies of carotenoid triplet formation in purple bacterial antenna complexes, J. Phys. Chem. B 105 (2001) 5525–5535.

[43] M. Di Valentin, S. Ceola, E. Salvadori, G. Agostini, D. Carbonera, Identification by Time-Resolved EPR of the peridinins directly involved in chlorophyll triplet quenching in the peridinin–chlorophyll a–protein from *Amphidinium carterae*, Biochim. Biophys. Acta Bioenerg. 1777 (2008) 186–195.